Electronic Supplementary Material (ESI) for Nanoscale.
This journal is © The Royal Society of Chemistry 2019

Electronic Supporting Information

Quantifying the effects of engineered nanomaterials on endothelial cell architecture and vascular barrier integrity using a cell pair model

Feyisayo Eweje,‡[a] Herdeline Ann M. Ardoña,‡[a] John F. Zimmerman,[a] Blakely B. O'Connor,[a] Seungkuk Ahn,[a] Thomas Grevesse,§[a] Karla N. Rivera,[a] Dimitrios Bitounis,[b] Philip Demokritou[b] and Kevin Kit Parker[a]*

a. Disease Biophysics Group, Wyss Institute for Biologically Inspired Engineering, John A. Paulson School of Engineering and Applied Sciences, Harvard University, Cambridge, MA 02138, USA. Email: kkparker@seas.harvard.edu

b. Center for Nanotechnology and Nanotoxicology, Department of Environmental Health, T. H. Chan School of Public Health, Harvard University, Boston, MA 02115, USA

‡ These authors contributed equally to this work.

§ Current address: Department of Biology, Concordia University, Montréal, QC H3G 1M8, Canada

Supplementary Methods

Quantification of endothelial cell pair features: For each coverslip sample, at least 10 islands with two cells each confined to a separate hexagon in the pattern were analyzed. Prior to analysis, each cell pair was centered and horizontally aligned; the original center and rotation angle of the cell pairs were determined from a thresholded FN stain image for each pair. The thresholded FN stain image was also used to measure the area of the FN island underlying each pair. Cell pair area was approximated by first enhancing the contrast of the F-actin stain image for each pair such that 50% of the pixels were saturated, then individually thresholding each image and measuring the area of the resulting shape. These area values were used to calculate the cell pair to FN island area ratio, as depicted in Figure 3a. Internuclear separation was measured by thresholding the DAPI stain image for each cell pair and determining the distance between the center locations of the two nuclei as illustrated in Figure 6b. Nuclear eccentricity, calculated as $\sqrt{1-\frac{b^2}{a^2}}$, was measured by fitting the nuclei to ellipses with semi-major and semi-minor axes, a and b, respectively.[1] The resulting values range from 0 to 1, where 0 is a circle.

Actin distribution maps were created by generating a composite image depicting the average intensity in each pixel location of a stack of centered F-actin stain images. Composites images were normalized such that 0.2% of pixels in the images appeared as saturated. Pixel color was assigned by applying the royal lookup table function, in which white depicts fully saturated pixels. Radial actin distribution was measured by collecting a radial profile originating from the center of each hexagon on the FN island. The red, dashed vertical lines at R = 26.86 μm and R = 31.02 μm shown in all radial distribution plots depict where the scan radius generates a circle inscribed in the hexagon and circumscribed around the hexagon, respectively. Central actin intensity ratio was calculated by averaging the ratios between the experimental and control pixel intensity values for every radial value along the profile. The average pixel intensity values for the control samples were normalized from 0 to 1, and the average intensity

values for the experimental samples were adjusted accordingly. Actin expression intensity in the cell-cell junction area was quantified by calculating the normalized mean pixel intensity along a linear profile created through the midline of the intercellular junction. The midline profile used to measure actin intensity at the junction was based on the VE-cadherin images as described below.

VE-cadherin expression at the junction of the two cells was determined by measuring the mean pixel intensity along a linear profile created through the midpoints of the junction width as determined visually (see Figure 7a). Prior to analysis, images were converted to 8-bit such that each image had a minimum and maximum pixel value of 0 and 255 respectively. The reported values are the average of the mean pixel intensities measured from $n \geq 20$ images and were normalized based on the unexposed sample value. Similarly, actin density along the intercellular junction area was quantified using the linear profile as defined via the corresponding VE-cadherin image. Finally, intercellular gap area was determined by selecting regions of interest within cell pair F-actin images to the areas where separation between the edges of the two cells were visible despite cell-cell contact being possible, thresholding the image, and calculating the total area of the observed particle(s). The sample size is reported as the total number of pairs analyzed.

Colocalization maps for vinculin and fibronectin: Quantiative analysis of vinculin colocalization with fibronectin was conducted using the colocalization threshold plugin in ImageJ. Images were converted to 8-bit prior to analysis. The Costes method was used to determine threshold pixel intensities for each channel, above which the two stains were labeled as colocalized.[2] The colocalization percentage is defined by calculating the Mander's colocalization coefficient (M), where 0 and 1 would indicate no and perfect colocalization respectively.[3]

$$M = \frac{\sum_i Vinculin_{i,colocalized}}{\sum_i Vinculin_i}$$

The denominator is the sum of the intensities of all pixels in the analyzed vinculin image that are above the threshold value. The numerator is the sum of the pixels within the aforementioned group that are located in positions where the corresponding pixel in the fibronectin or actin image also has an intensity above the threshold value for that channel.

Colocalized pixel images were generated by plotting the mean pixel intensity of the two analyzed channels. The radial distribution of colocalized vinculin-fibronectin pixels was measured by collecting a radial profile of these images originating from the center of each hexagon on the FN island for the analyzed pair, similar to those performed for actin distribution profiles. Relative peripheral intensity for vinculin-FN colocalized pixels is reported as the mean ratio between the exposed and unexposed average pixel intensities for all radius values.

Peripheral vinculin expression quantification: Peripheral vinculin expression was quantified using a method similar to that used to analyze cell pair actin distribution. As opposed to collecting a normalized radial distribution of pixel intensities from each analyzed image, raw pixel intensity values were measured from R = 15.5 μm (i.e. midway between the center and outermost edge of each hexagon composing the islands) to R = 26.86 μm (i.e. the radius of a circle inscribed in the hexagons). In addition, scans were conducted only on the outer half of each side of the islands to avoid non-specific staining in the central region. Relative peripheral vinculin expression is reported as the mean ratio between the exposed and unexposed average pixel intensities for all radius values.

Calculation of the "similarity index": The similarity index was used to quantitatively compare endothelial cell pairs exposed to Ag, TiO_2, CNC, and to unexposed controls. The index is a modified implementation of the Hellinger distance formula, which is used to quantify the similarity between two probability distributions. The index uses the mean (μ) and standard deviation (σ) values of measurements from unexposed and exposed cell pairs to calculate the separation between the probability distributions for each experimental parameter: cell pair/FN

island area ratio, central actin intensity ratio, VE-cadherin expression intensity, and mean intercellular gap size.

$$Score = 100 \times \left(\sqrt{\frac{2\sigma_{no\ ENM}\sigma_{with\ ENM}}{{\sigma_{no\ ENM}}^2 + {\sigma_{with\ ENM}}^2}} e^{-\frac{(\mu_{no\ ENM} - \mu_{with\ ENM})^2}{4\,({\sigma_{no\ ENM}}^2 + {\sigma_{with\ ENM}}^2)}} \right)$$

The index score falls between 0 and 100, where a score of 0 indicates that the distributions are completely different (*i.e.*, no match between the exposed and unexposed cell pairs for that condition) and a score of 100 indicates a completely similar data distribution (*i.e.*, a complete match between the exposed and unexposed cell pairs for that condition). Combined scores for each condition were calculated as the mean score for the four evaluated parameters.

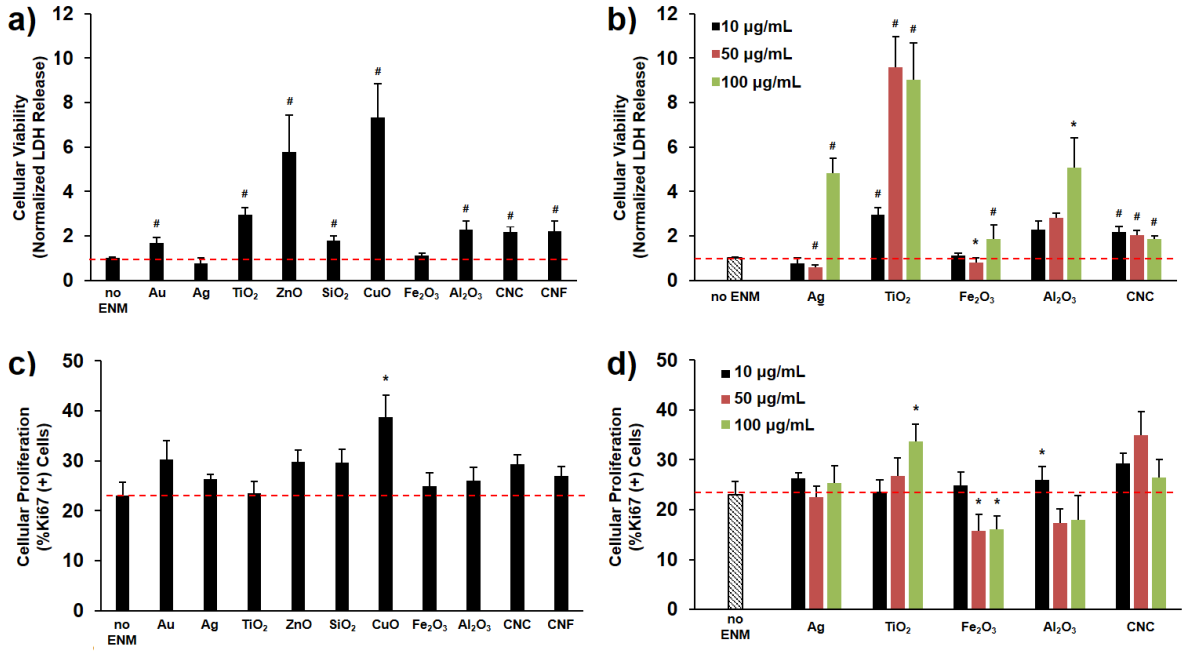

Figure S1. (a,b) Lactate dehydrogenase (LDH) release and (c,d) Ki67 expression of pleomorphic HUVECs exposed to different ENMs for 24 h, normalized against the unexposed (no ENM) condition. Error bars represent standard error, $n \leq 3$ per exposure condition for LDH assay and $n \leq 5$ and Ki67 assay, where n is the number of wells per exposure condition. The red dashed lines represent the value for no ENM condition. For statistical comparison, *p <0.05, #p <0.001 with respect to control (no ENM).

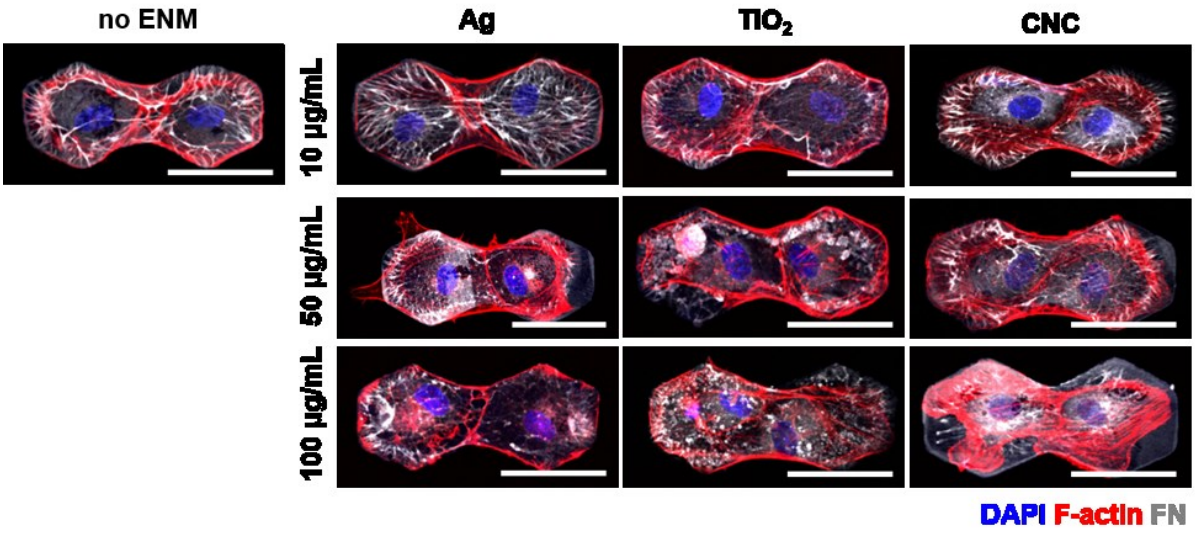

Figure S2. Representative confocal images of cell pairs on FN islands following 24 h exposure to Ag, TiO_2, and CNC. Scale bars = 50 µm.

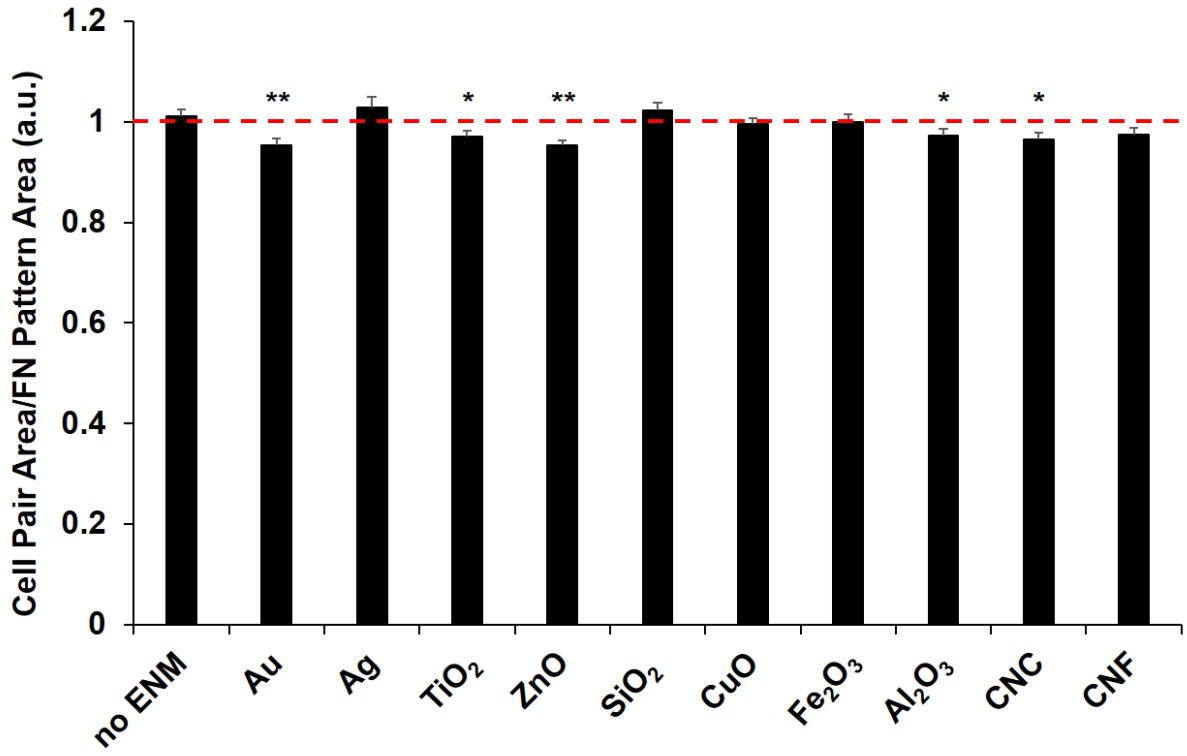

Figure S3. Cell pair-to-FN island area ratio (AR) following exposure to ENMs at 10 µg/mL ($n \geq 20$, where n is the number of cell pairs per exposure condition). Red dashed line represents the value for no ENM condition. For statistical comparison, *p <0.05, **p <0.005 with respect to control (no ENM).

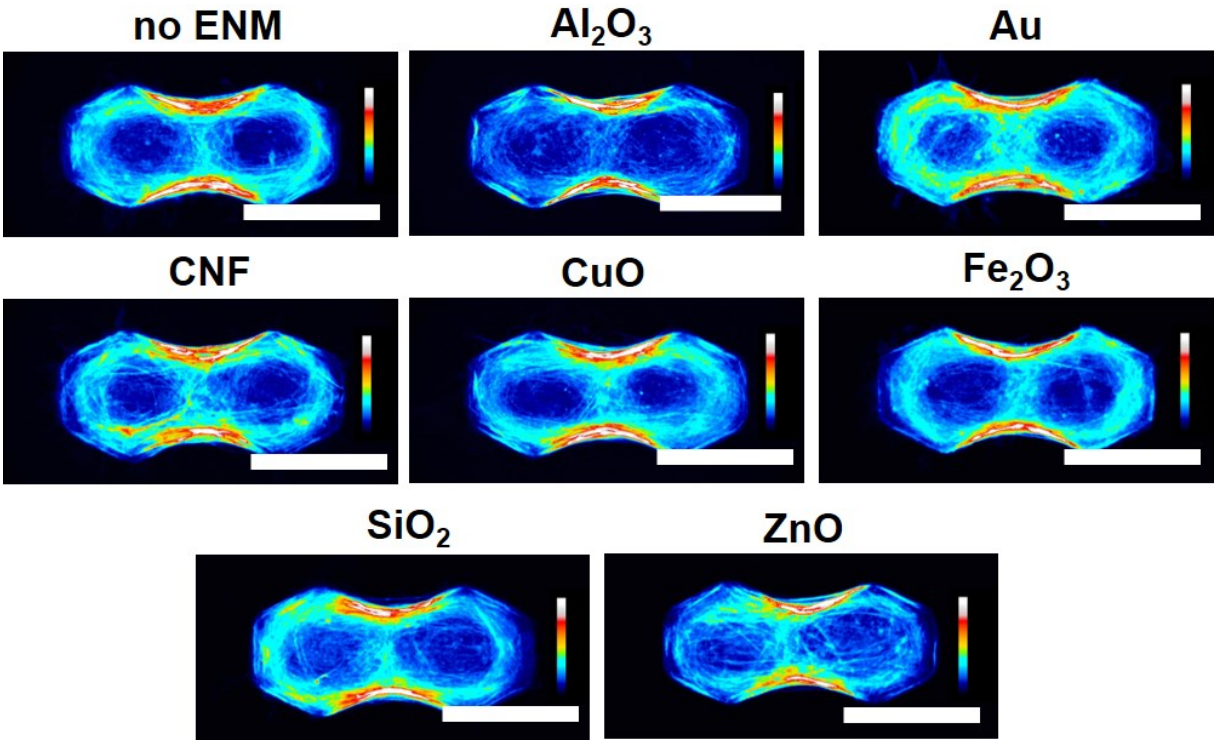

Figure S4. Composite confocal images of cell pairs under different ENM exposure conditions (no ENM and 7 ENMs at 10 μg/mL), immunostained against F-actin. Scale bars= 50 μm; $n \geq 20$ per composite heat map, where n is the number of cell pairs per exposure condition.

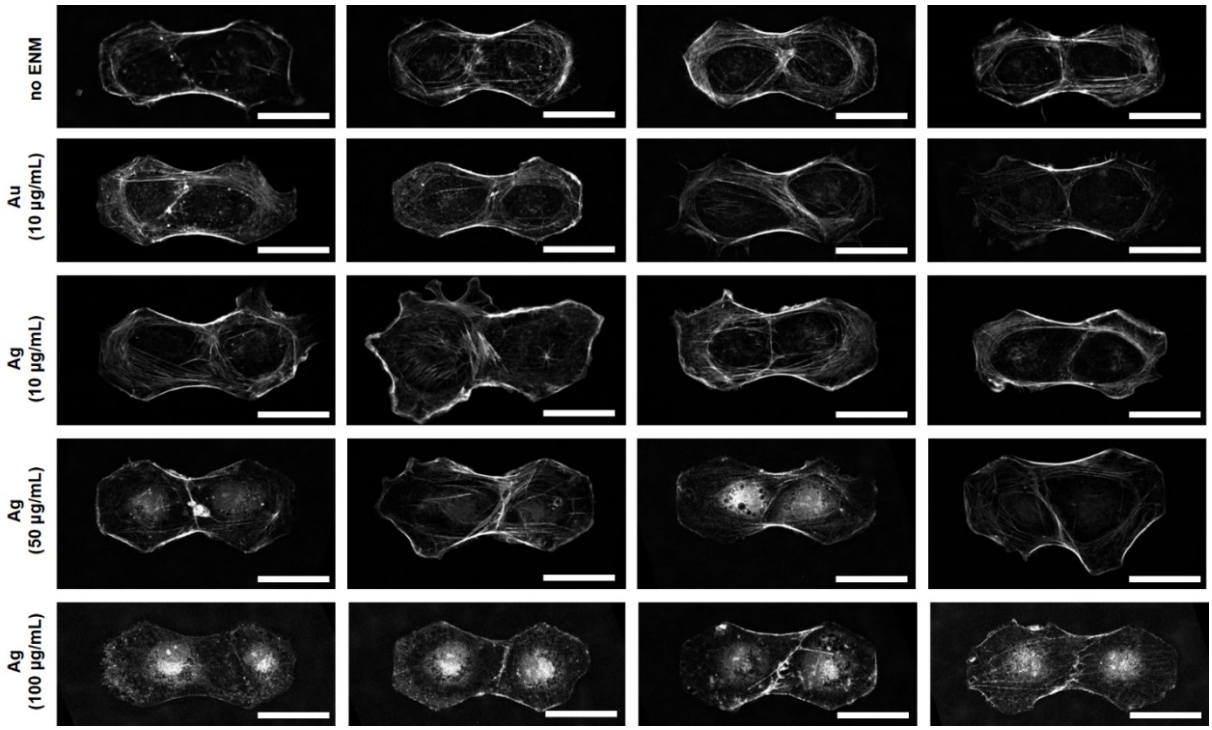

Figure S5. Representative confocal images of cell pairs immunostained against F-actin. Shown here are the following selected ENM exposure conditions: no ENM, Au at 10 µg/mL, and Ag at 10, 50 and 100 µg/mL. These images were used to create the composite maps presented in Figure 4 and Supplementary Figure 4. Scale bars= 50 µm; showing n =4 out of $n \geq 20$ used for the composite heat map, where n is the number of cell pairs per exposure condition.

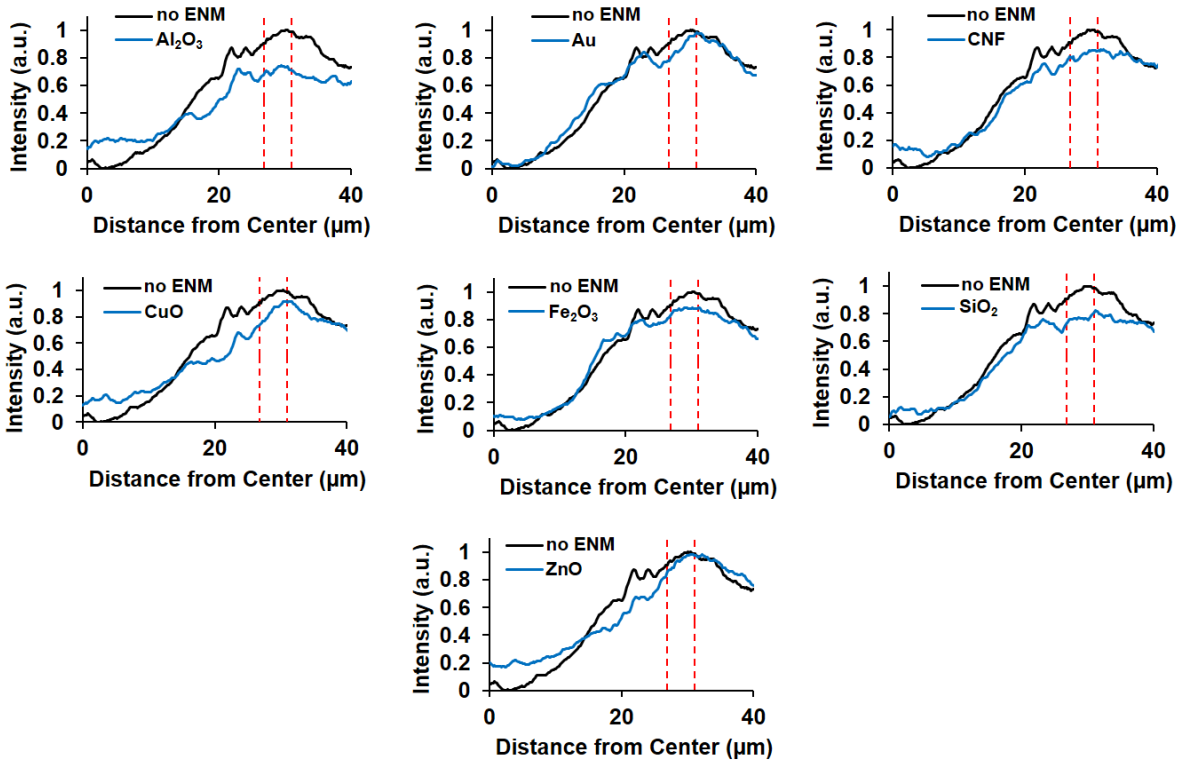

Figure S6. Average plots of radial actin distribution in endothelial cell pairs following ENM exposure at 10 μg/mL. The distribution is reported as normalized pixel intensity. Each cell in a pair was individually scanned from the center of its hexagonal island outward. The dashed red lines denote the radius of a circle inscribed (R = 26.86 μm) and circumscribed (R = 31.02 μm) in a single FN island hexagon; $n \geq 40$ (≥ 20 pairs, 2 scans per pair).

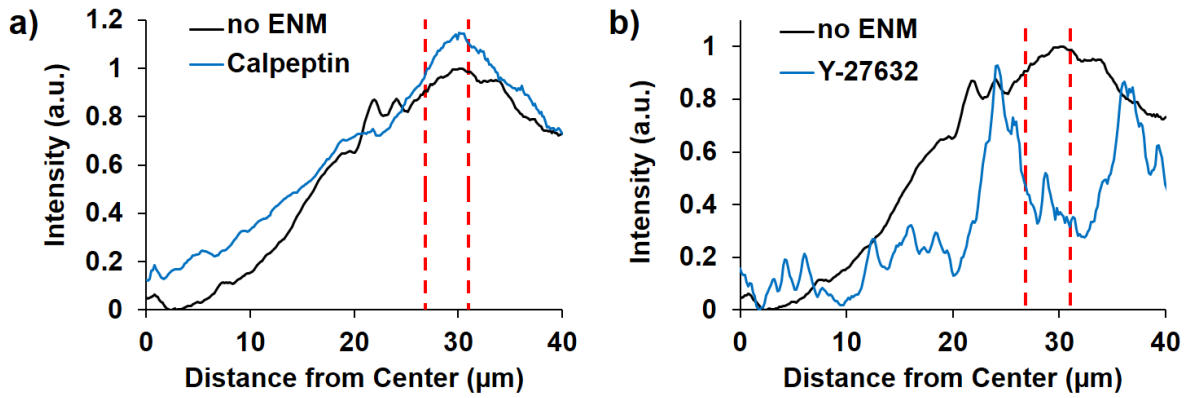

Figure S7. Average plots of radial actin distribution in endothelial cell pairs following exposure to cytoskeleton-modulating drugs, (a) calpeptin and (b) Y-27632. The distribution is reported as normalized pixel intensity. Each cell in a pair was individually scanned from the center of its hexagonal island outward. The dashed red lines denote the radius of a circle inscribed (R = 26.86 μm) and circumscribed (R = 31.02 μm) in a single FN island hexagon; $n \geq 20$ (≥ 10 pairs, 2 scans per pair).

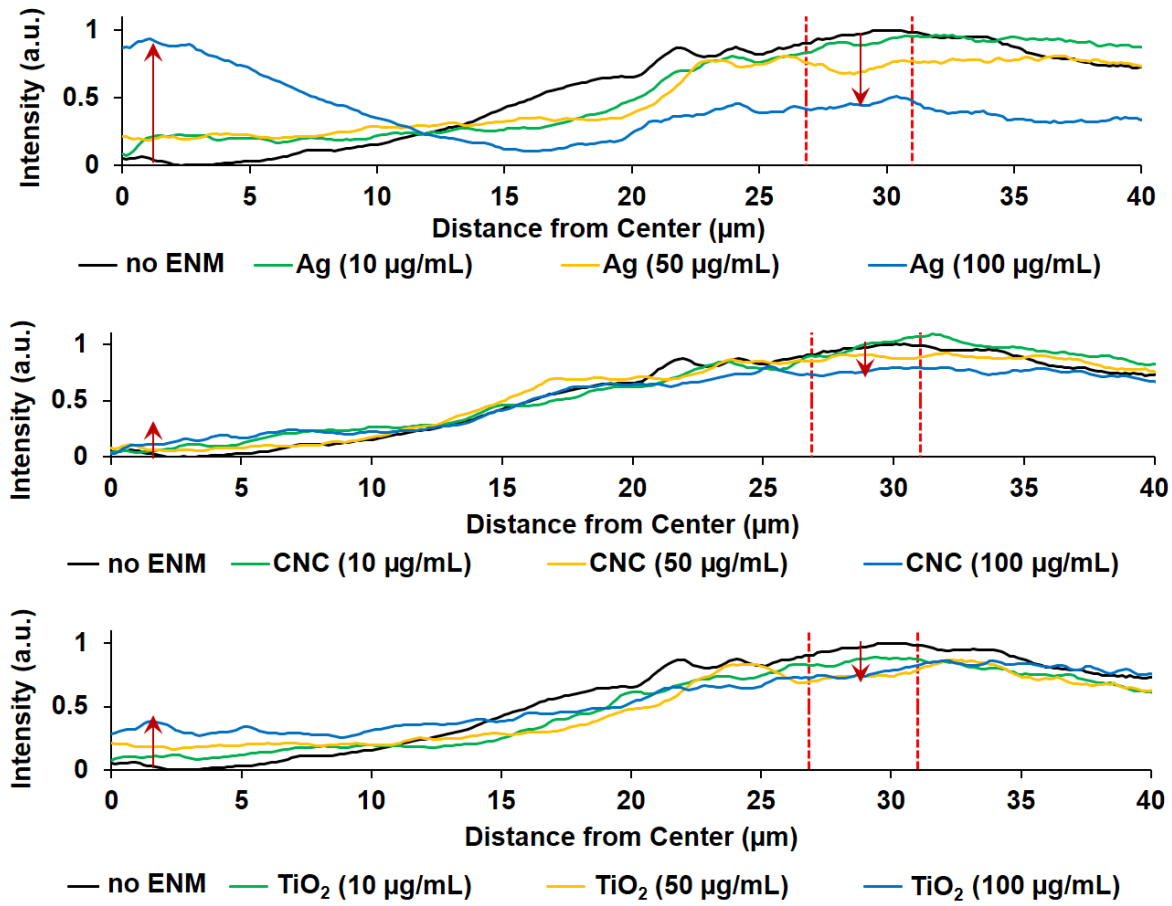

Figure S8. Average plots of radial actin distribution in endothelial cell pairs following exposure to Ag, TiO_2, and CNC at 10, 50, and 100 μg/mL. The distribution is reported as normalized pixel intensity. Each cell in a pair was individually scanned from the center of its hexagonal island outward. Red arrows indicate the general trend as the ENM dose increases from 0 to 100 100 μg/mL. The dashed red lines denote the radius of a circle inscribed (R = 26.86 μm) and circumscribed (R = 31.02 μm) in a single FN island hexagon. $n \geq 40$ (≥ 20 pairs, 2 scans per pair).

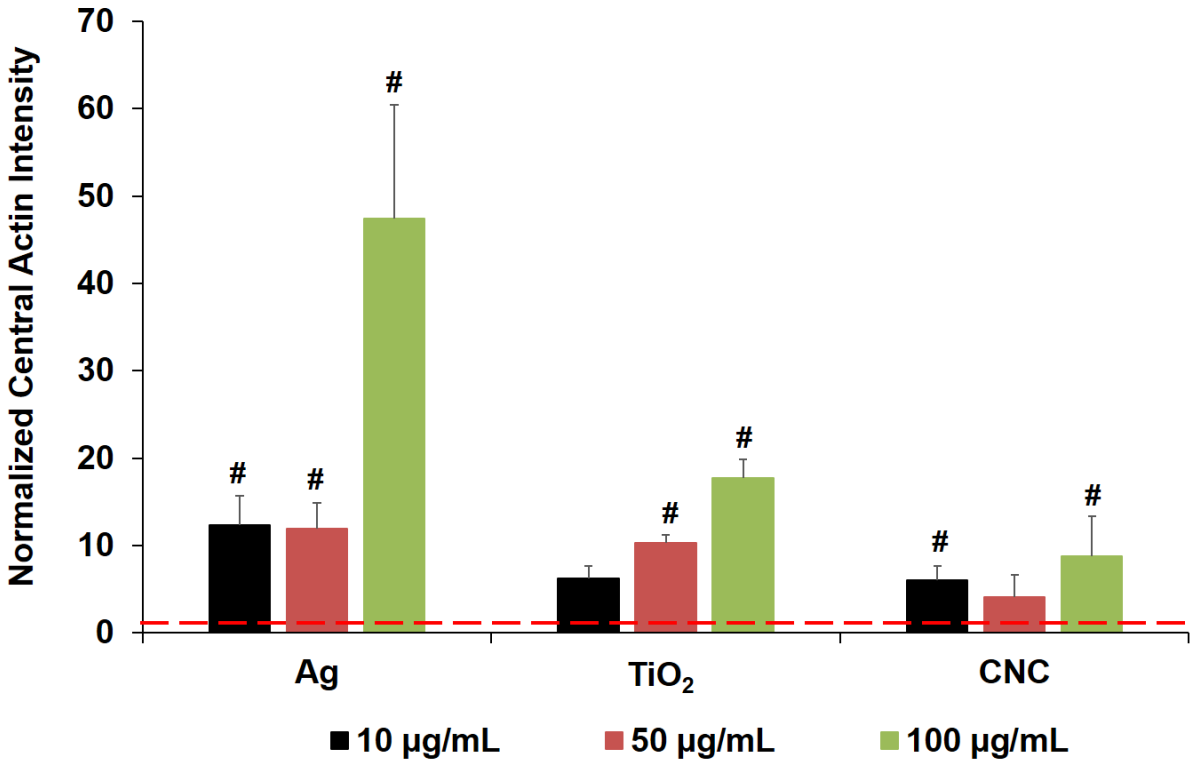

Figure S9. Quantification of actin distribution in the central region (0 to 15.5 µm from the center of 1 hexagon) of ENM-exposed patterned cells using radial scanning; normalized against the values for unexposed cell pairs ($n \geq 20$, where n = total number of pairs observed for each condition). The red dashed line represents the value for no ENM condition. For statistical comparison, #p <0.001 with respect to control (no ENM).

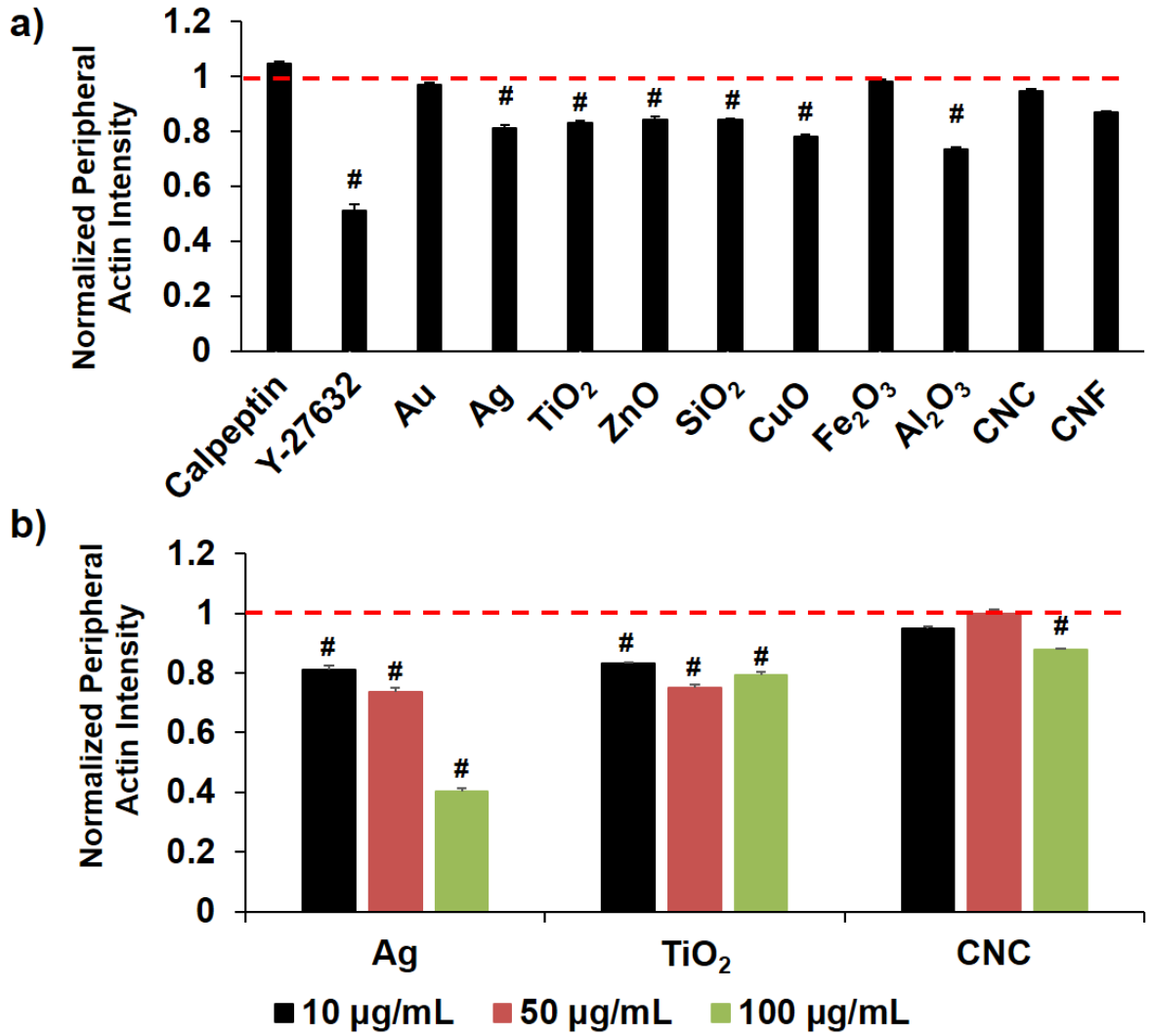

Figure S10. Quantification of actin distribution in the peripheral region (15.5 to 31 µm from the center of 1 hexagon) of cell pairs following exposure to ENMs at (a) 10 µg/mL and (b) 10, 50, and 100 µg/mL. Measurements for cell pairs treated with cytoskeleton modulating drugs, calpeptin (Rho activator) and Y-27632 (ROCK inhibitor), are also shown in (a). Values are normalized against the values for unexposed cell pairs ($n \geq 20$, where n = total number of pairs observed for each condition). The red dashed lines represent the value for no ENM condition. For statistical comparison, #p <0.001 with respect to control (no ENM).

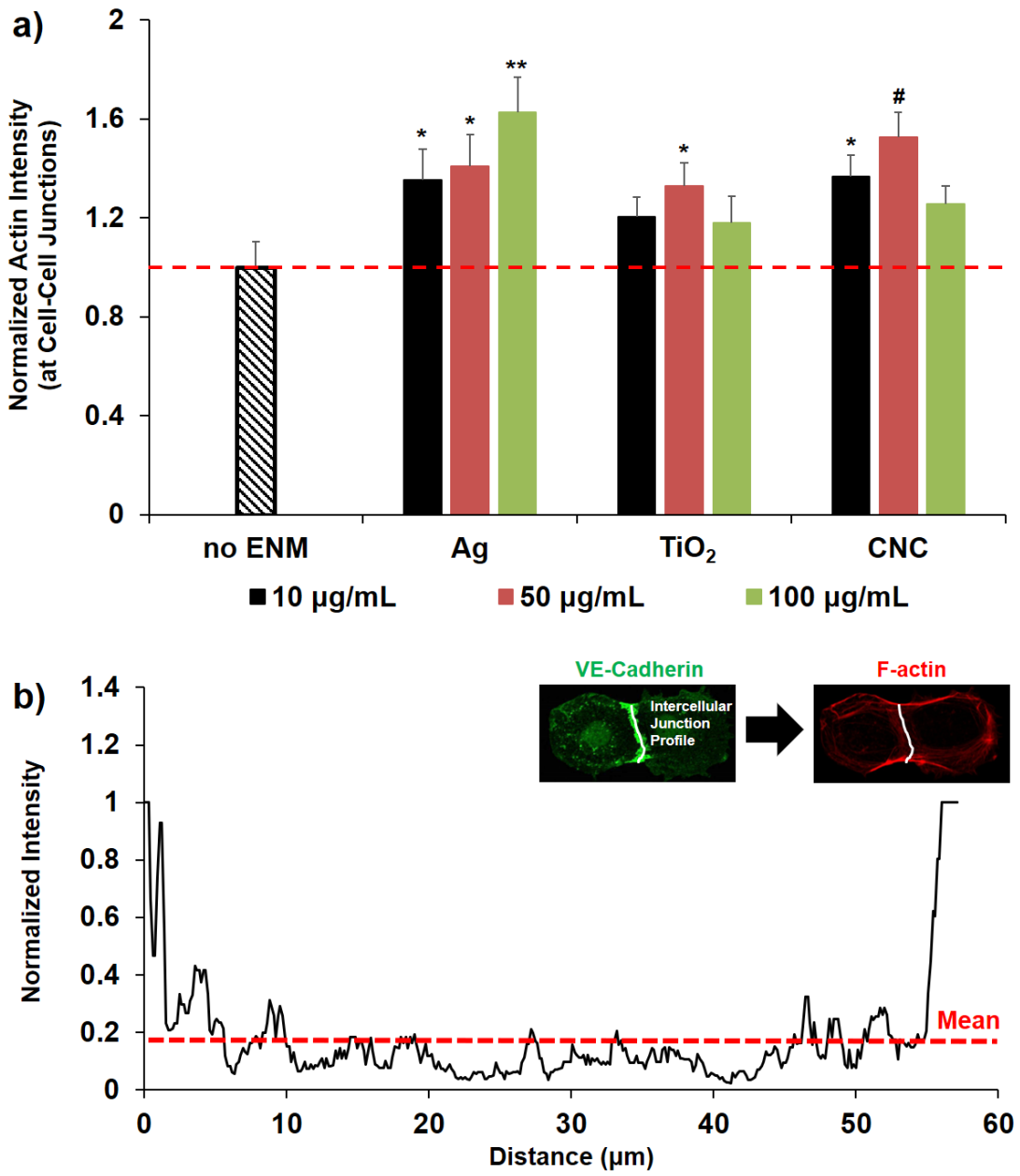

Figure S11. (a) Actin intensity at the cell-cell junction region of cell pairs (36 to 163 µm in length across all pairs) following exposure to ENMs at 0, 10, 50, and 100 µg/mL of Ag, TiO_2 and CNC. All measurements were normalized against the values for unexposed cell pairs ($n \geq 20$, where n = total number of pairs observed for each condition). The red dashed lines represent the value for no ENM condition. For statistical comparison, *p <0.05, **p <0.005 , #p <0.001 with respect to control (no ENM). (b) Representative actin intensity plot along the junction area of a cell pair to determine a mean intensity value. Inset: Example images demonstrating that the midline of the junction area per cell pair was determined using the VE-cadherin image, which was then applied to the F-actin image to measure actin intensity at the cell-cell junction region.

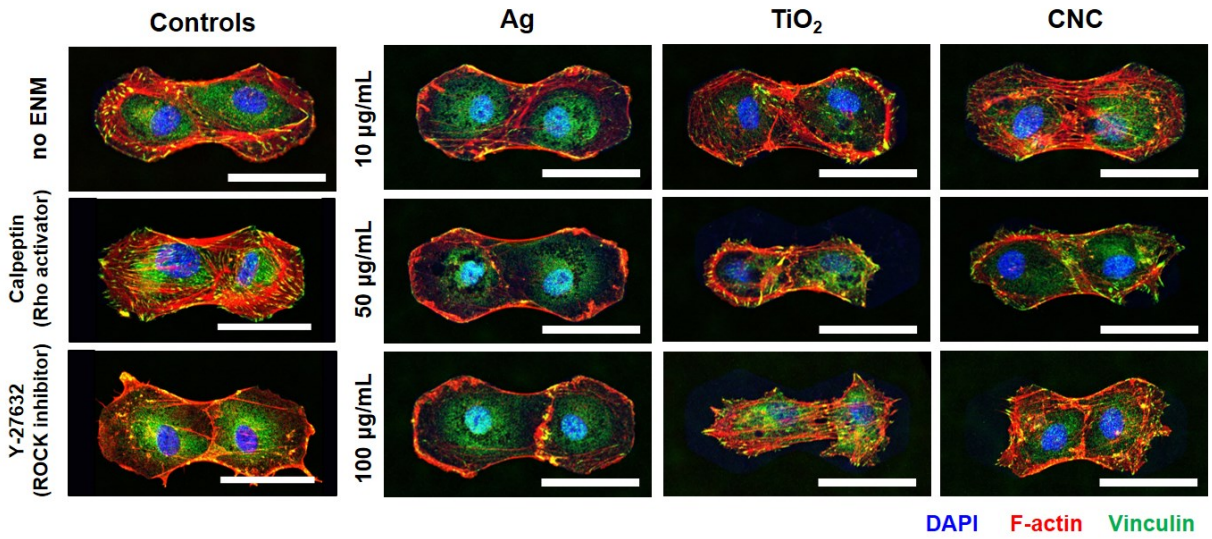

Figure S12. Representative confocal images of cell pairs on FN islands, showing staining for vinculin, after 24 h exposure to Ag, TiO_2, CNC and cytoskeleton modulating drugs. Scale bars = 50 µm.

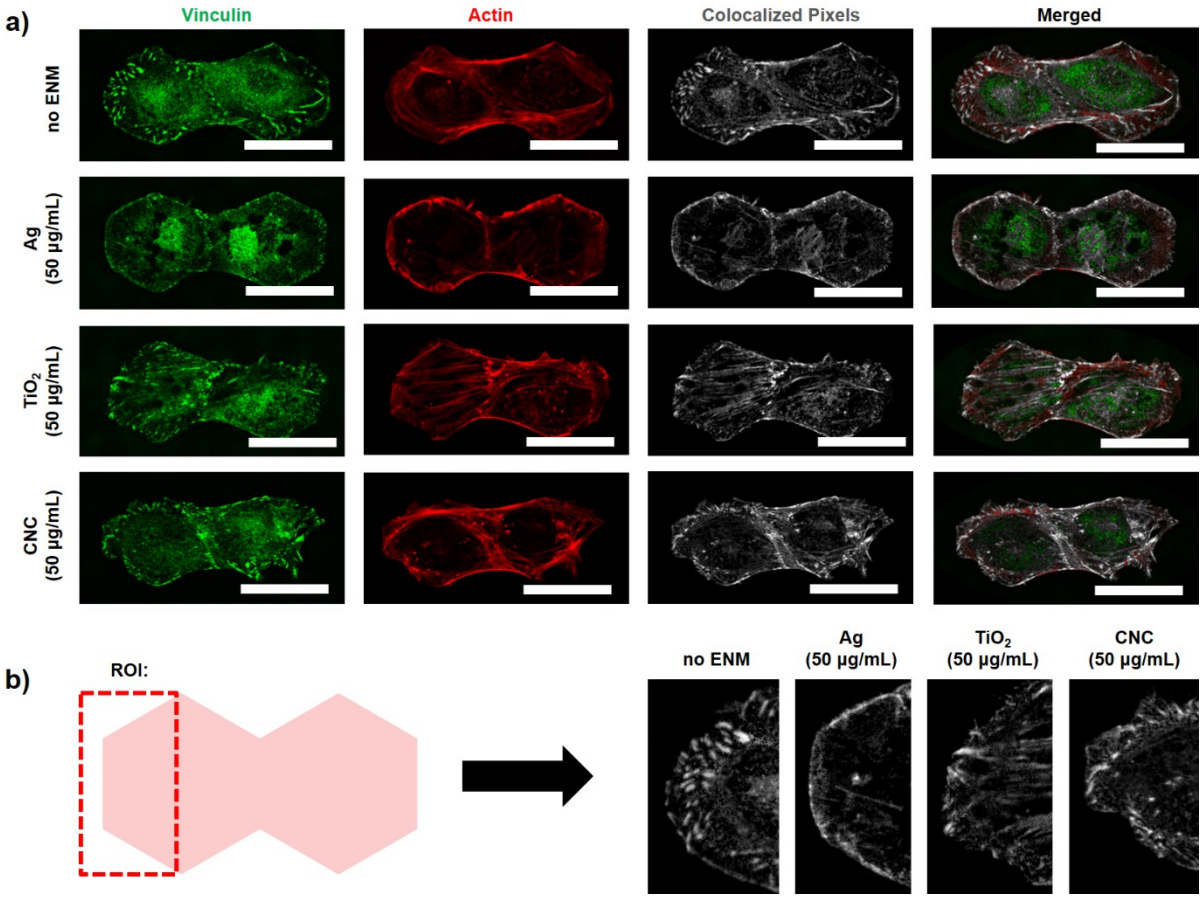

Figure S13. (a) Representative images of cell pairs exposed to Ag, TiO_2 and CNC at 0 and 50 µg/mL, immunostained against vinculin and actin. Colocalization of vinculin and actin pixels as defined by Costes method. Scale bars=50 µm; $n \geq 10$, where n is the number of cell pairs per exposure condition. (b) Images showing the colocalized actin and vinculin pixels per representative image in (a), focusing on a region of interest (ROI) at a cell pair edge.

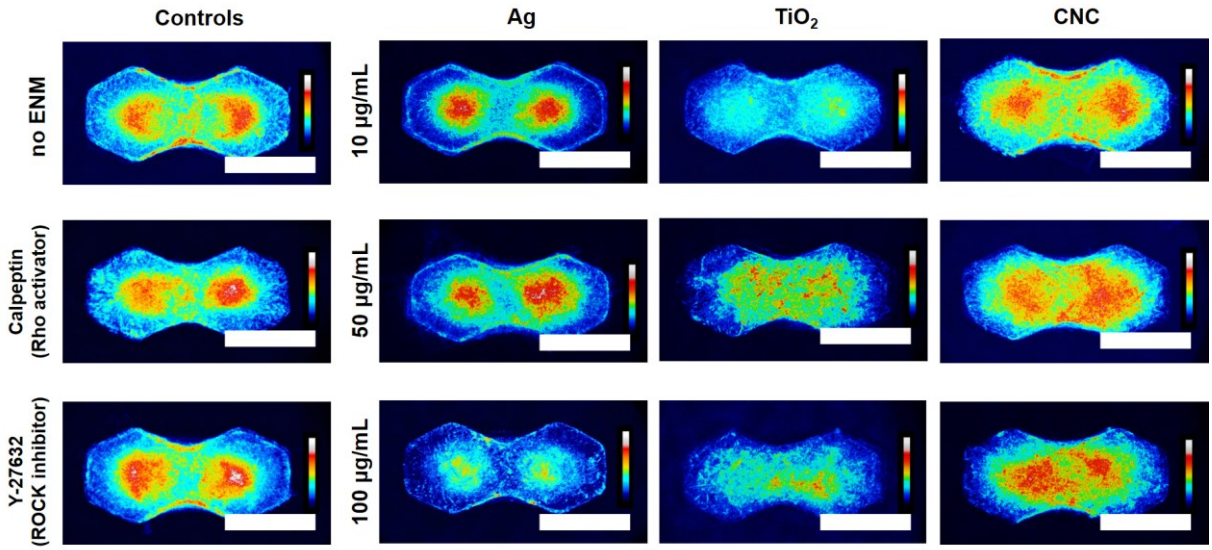

Figure S14. Composite confocal images of cell pairs exposed to Ag, TiO_2 and CNC at 0, 10, 50, 100 µg/mL, and to cytoskeleton modulating drugs, immunostained against vinculin. Scale bars=50 µm; $n \geq 10$ per composite heat map, where n is the number of cell pairs per exposure condition.

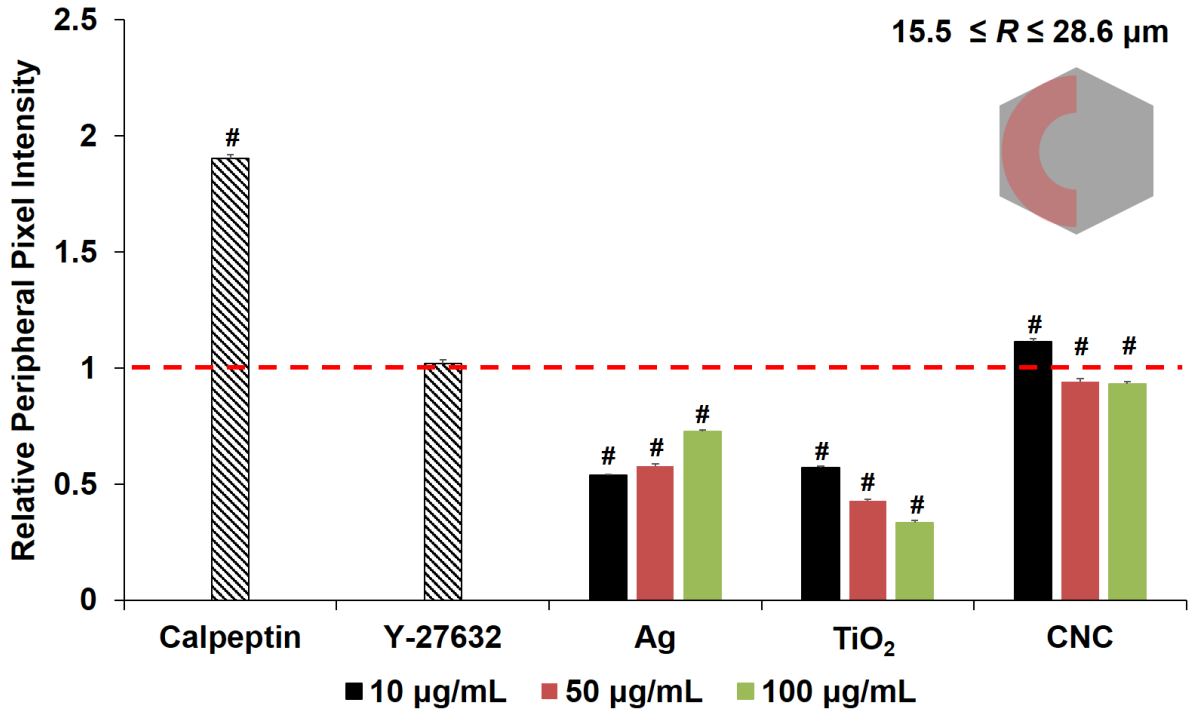

Figure S15. Peripheral (R = 15.5 µm to 26.86 µm) vinculin pixel intensity relative to unexposed samples. Inset: Scans were conducted on the outer half of each side of the islands to avoid non-specific staining in the central region; R = 26.86 µm is the radius of a circle inscribed in a single FN island hexagon. $n \geq 10$; for statistical comparison, #$p < 0.001$.

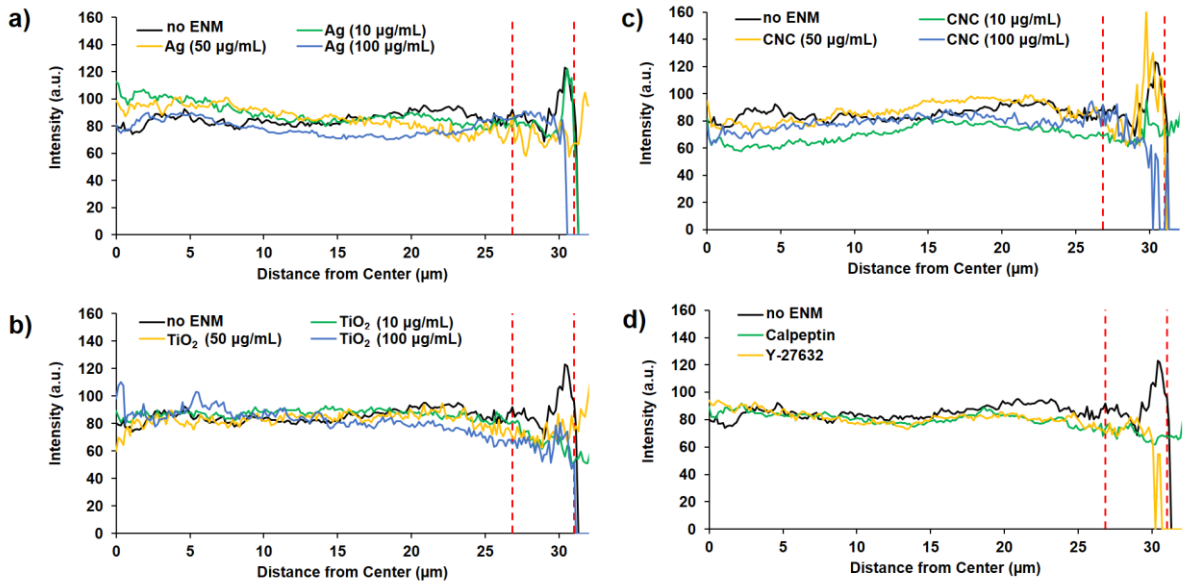

Figure S16. Average plots of radial distribution of colocalized vinculin and fibronectin in endothelial cell pairs, following exposure to (a-c) ENMs (Ag, TiO_2, and CNC at 10, 50, and 100 µg/mL) and (d) drug controls (calpeptin and Y-27632). The distribution is reported as normalized pixel intensity with respect to no ENM condition. Scans were conducted on the outer half of each side of the islands to avoid non-specific staining in the central region; $15.5 \leq R \leq 26.86$ µm. The dashed red lines denote the radius of a circle inscribed ($R = 26.86$ µm) and circumscribed ($R = 31.02$ µm) in a single FN island hexagon. $n \geq 20$ (≥ 10 pairs, 2 scans per pair).

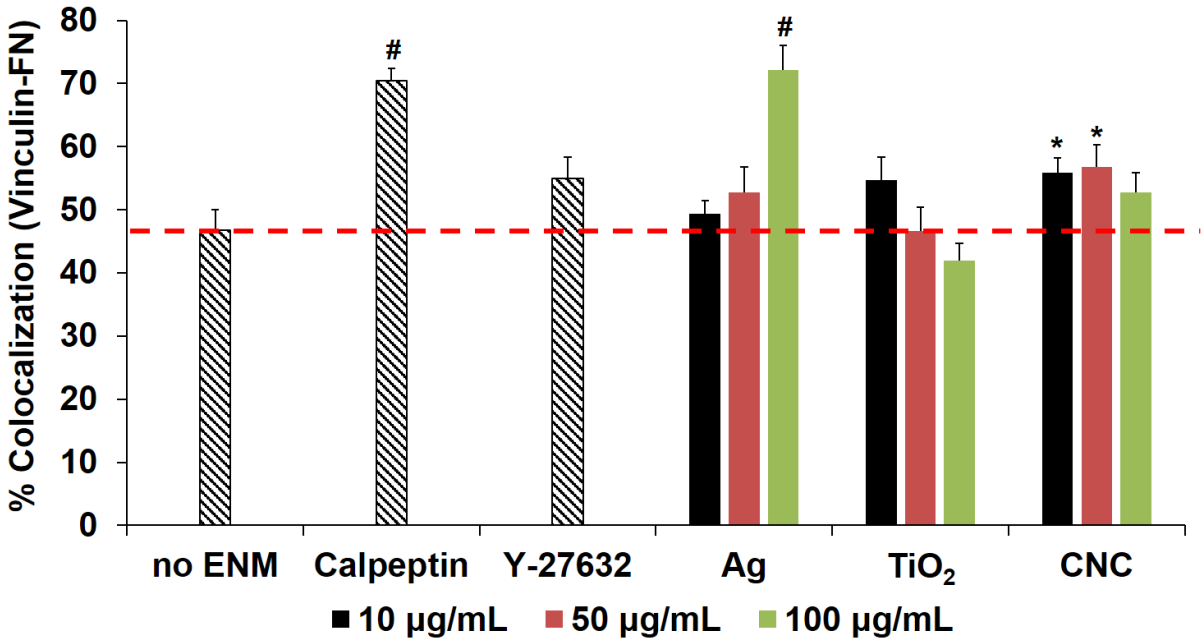

Figure S17. Colocalization percentage of vinculin and fibronectin pixels (with respect to total vinculin pixels) for cell pairs exposed to ENMs at different doses and to cytoskeleton-modulating drugs (calpeptin and Y-27632). Percentage of colocalized pixels were calculated using the Mander's colocalization coefficient; $n \geq 10$, where n is the number of cell pairs analyzed per exposure condition.

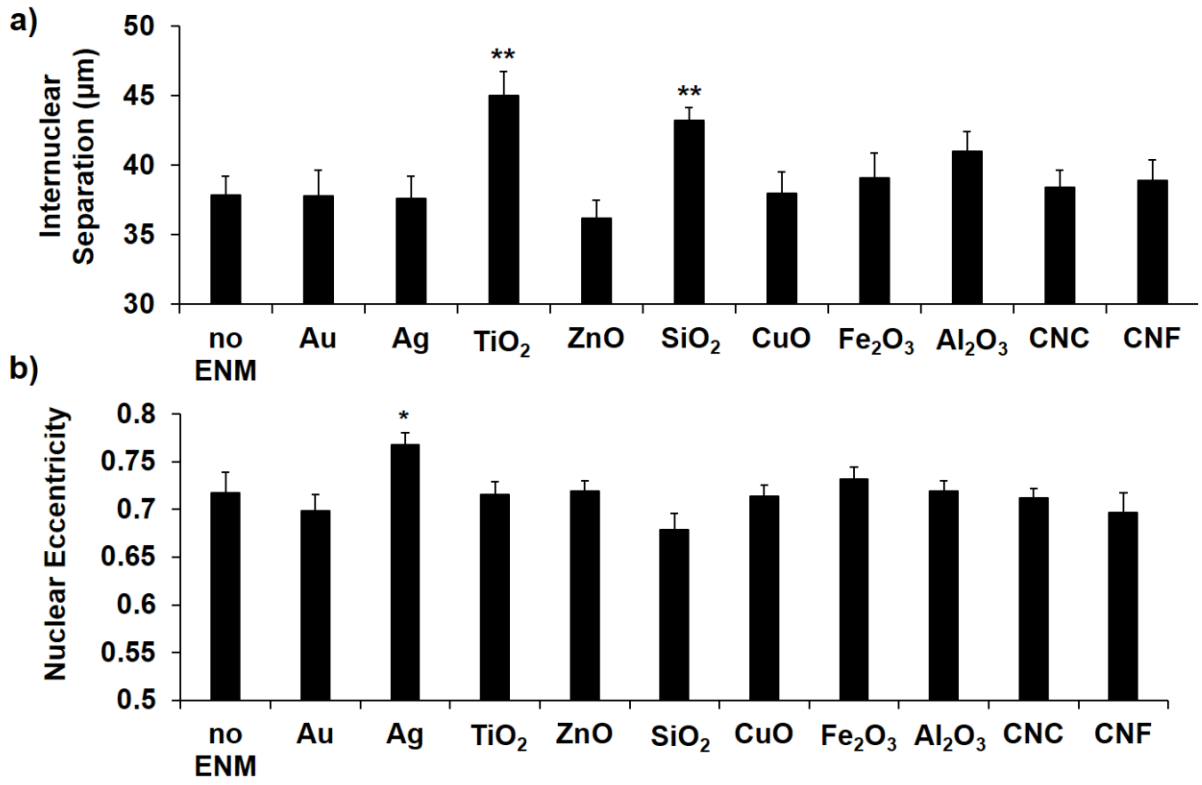

Figure S18. (a) Internuclear separation and (b) nuclear eccentricity of endothelial cell pairs following exposure to ENMs at 10 μg/mL ($n \geq 20$, where n is the number of cell pairs per exposure condition). For statistical comparison, *$p < 0.05$, **$p < 0.005$ with respect to no ENM condition.

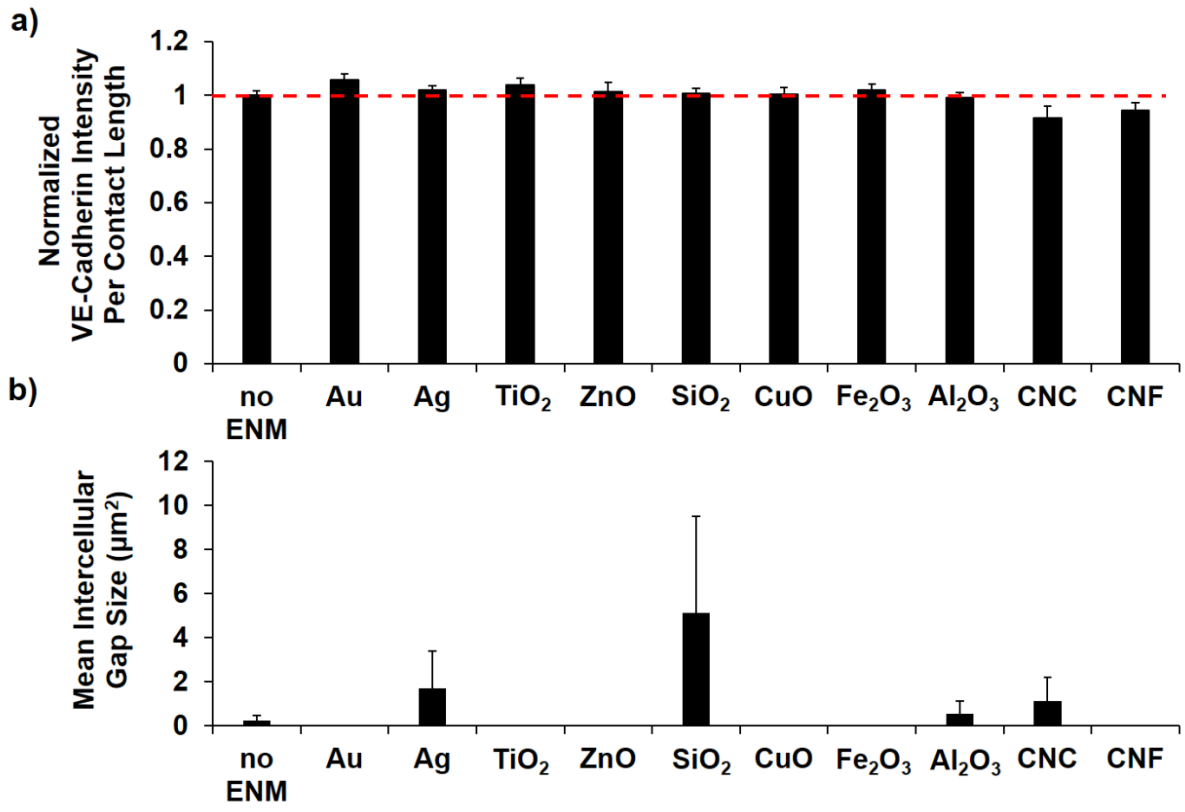

Figure S19. (a) VE-cadherin expression intensity and (b) mean intercellular gap size following exposure to ENMs at 10 μg/mL ($n \geq 20$, where n is the number of cell pairs per exposure condition). The red dashed line represents the value for no ENM condition.

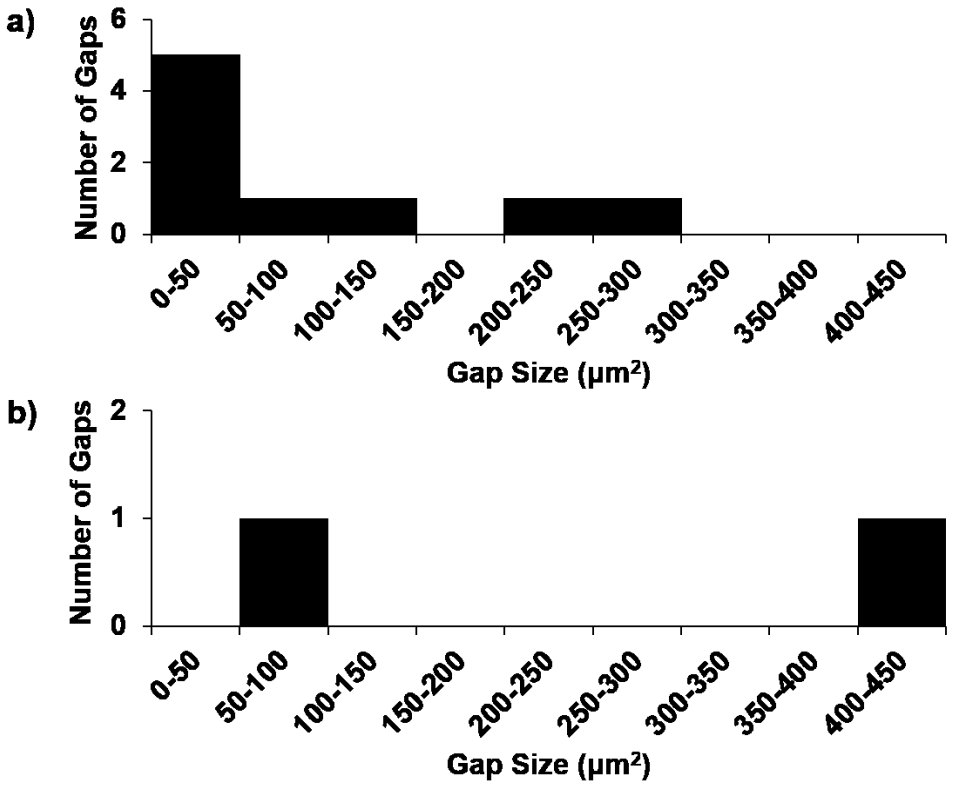

Figure S20. Histogram of gap sizes for endothelial cell pairs exposed to (a) Ag and (b) TiO_2 at 100 μg/mL (n = 21 for Ag; n = 20 for TiO_2), where n is the number of cell pairs per exposure condition). Cell pairs that did not show any gaps greater than 2 μm^2 were excluded from the histogram.

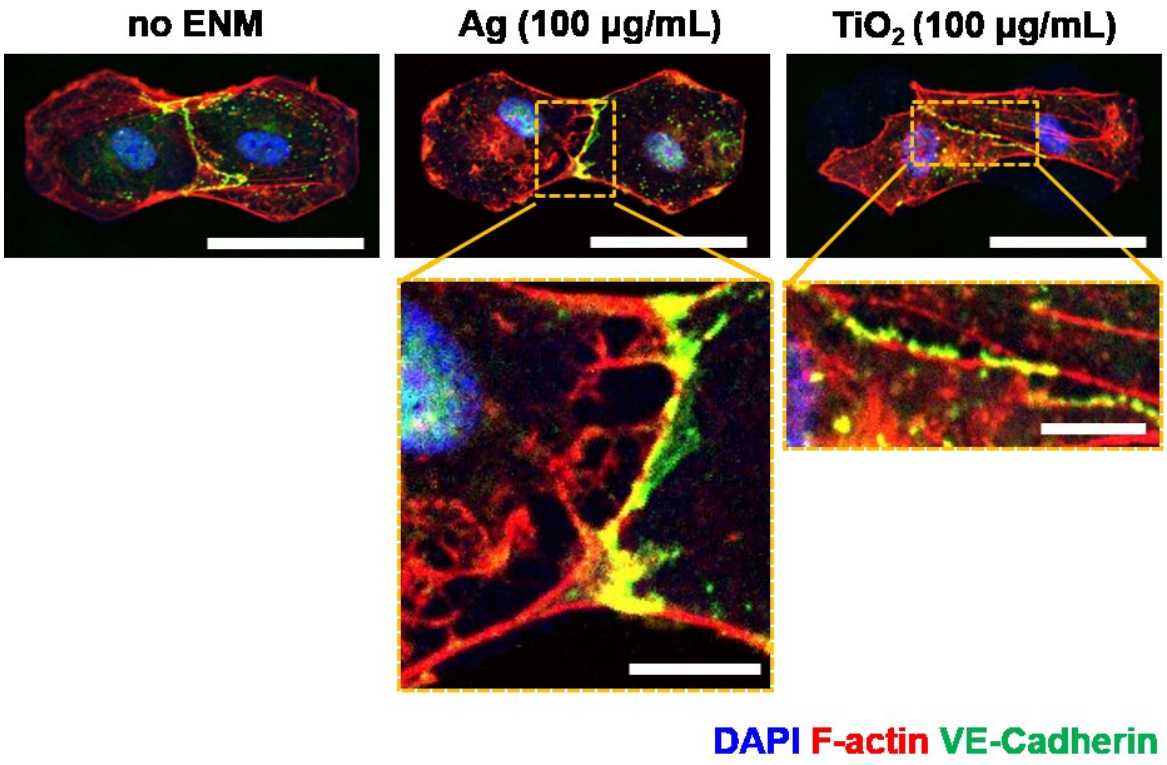

Figure S21. Representative confocal images of cell pairs with intercellular gaps following exposure to Ag and TiO_2 at 100 µg/mL. Scale bars= 50 µm (10 µm on magnified images).

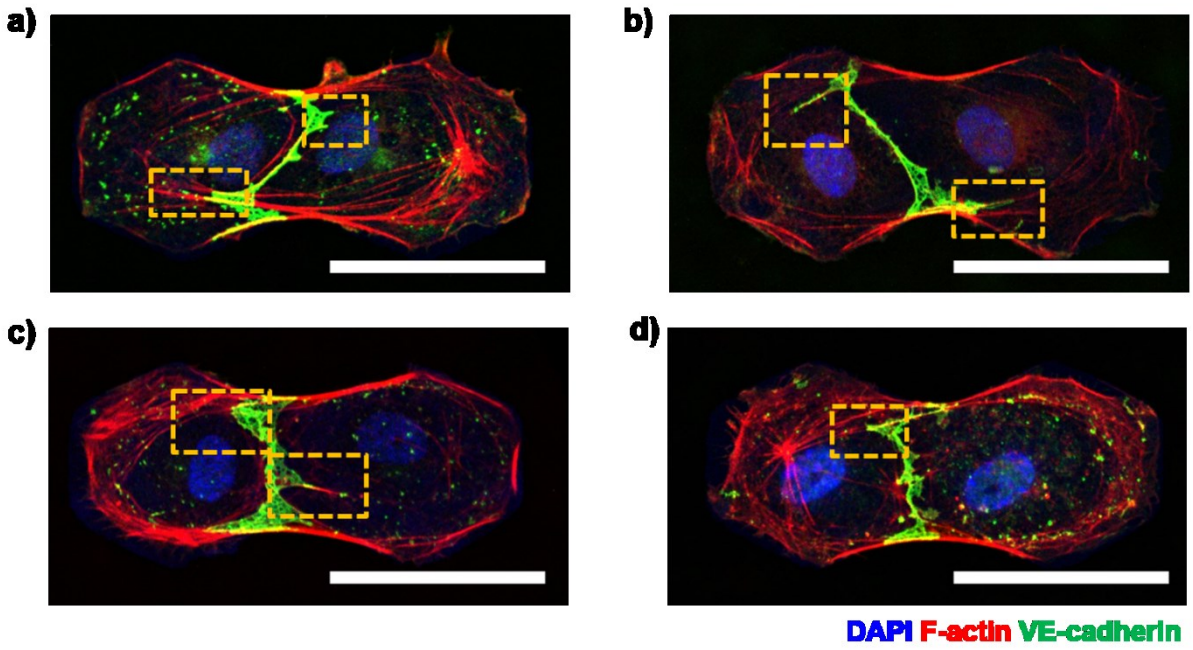

Figure S22. Examples of discontinuous adherens junctions in HUVEC pairs following exposure to a) Ag NPs at 10 µg/mL, b) Ag NPs at 50 µg/mL, c) TiO_2 NPs at 10 µg/mL, and d) TiO_2 NPs at 50 µg/mL. Scale bars= 50 µm.

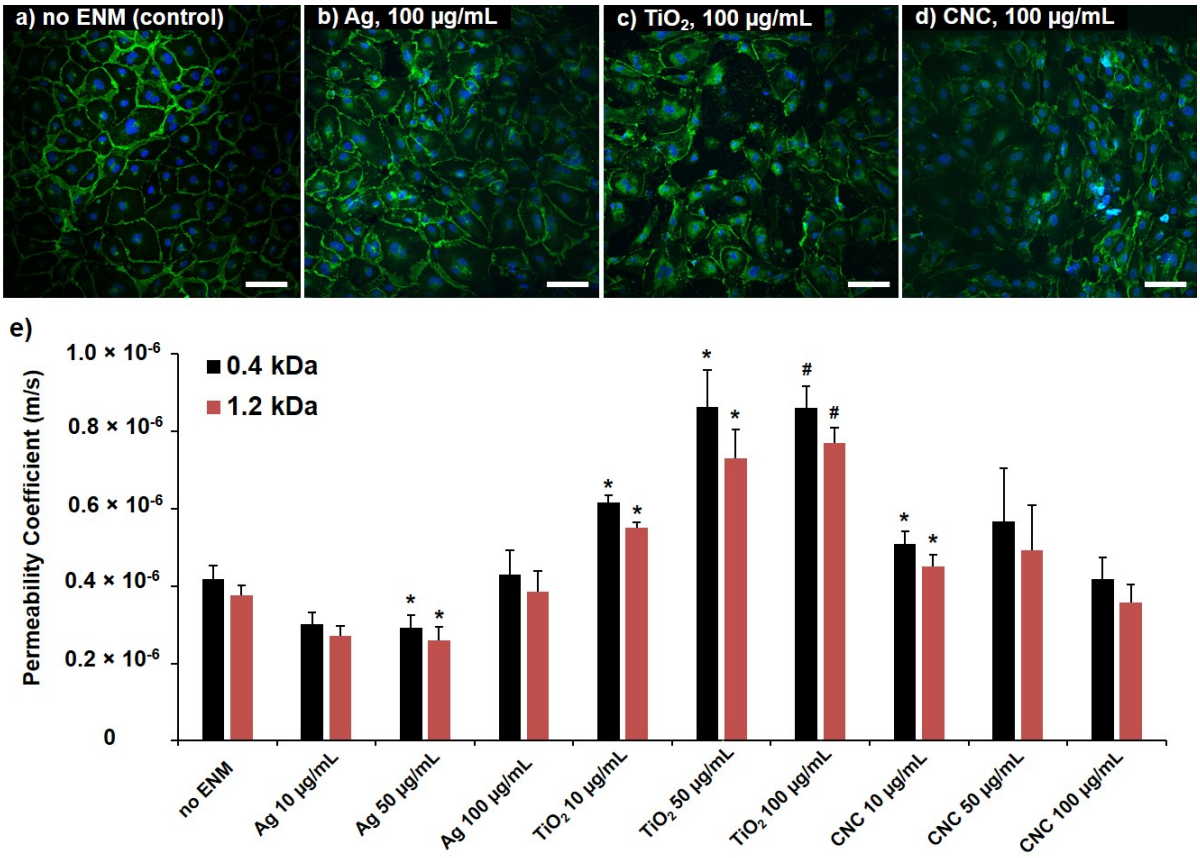

Figure S23. (a-d) Representative images of HUVEC monolayers grown on Transwell polyester membranes coated with fibronectin under different exposure conditions; scale bars= 50 µm. (e) Measured permeability coefficients of HUVEC monolayers ($n \geq 3$, where n is the number of wells per exposure condition) 24 hours post-exposure to Ag, TiO_2 and CNC at 10, 50 and 100 µg/mL. For statistical comparison against the unexposed HUVEC monolayers (no ENM): *$p <$ 0.05, #$p < 0.001$.

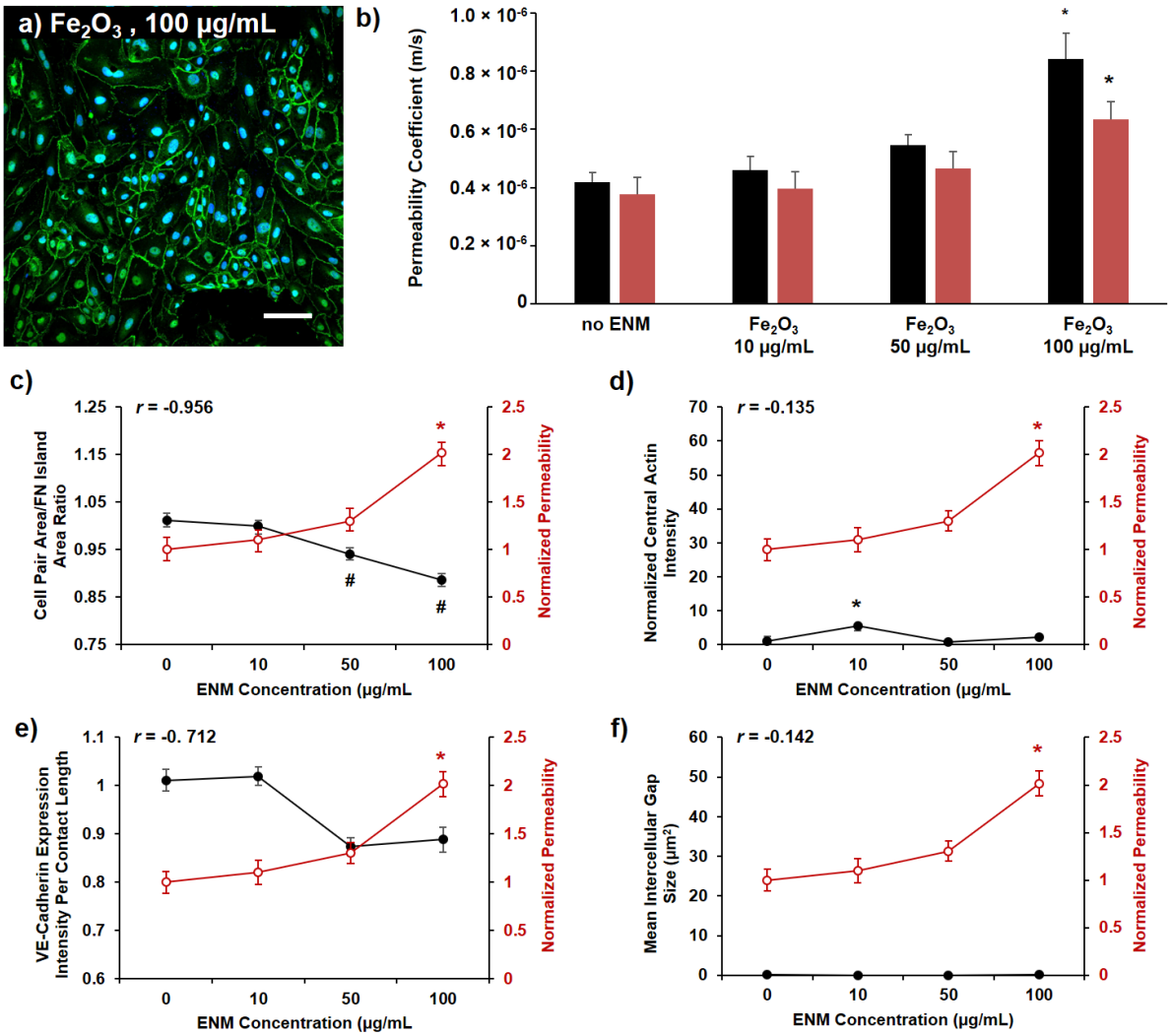

Figure S24. (a) Representative image of HUVEC monolayers grown on Transwell polyester membranes coated with fibronectin, exposed to 100 µg/mL Fe_2O_3; scale bar= 100 µm. (b) Measured permeability coefficients of HUVEC monolayers (n= 9, where n is the number of wells per exposure condition) 24 hours post-exposure to Fe_2O_3 at 10, 50 and 100 µg/mL. (c-f) Correlation plots between changes in structural parameters measured using the cell pair model and endothelial monolayer permeability. (c) Cell pair-to-FN island area ratio, (d) central actin intensity ratio, (e) VE-cadherin expression intensity in intercellular junction area, and (f) mean intercellular gap size (black curves) plotted with normalized endothelial monolayer permeability (red curves, normalized with respect to unexposed conditions) as a function of ENM exposure level. For statistical comparison against the unexposed HUVEC monolayers (no ENM): *$p < 0.05$, #$p < 0.001$.

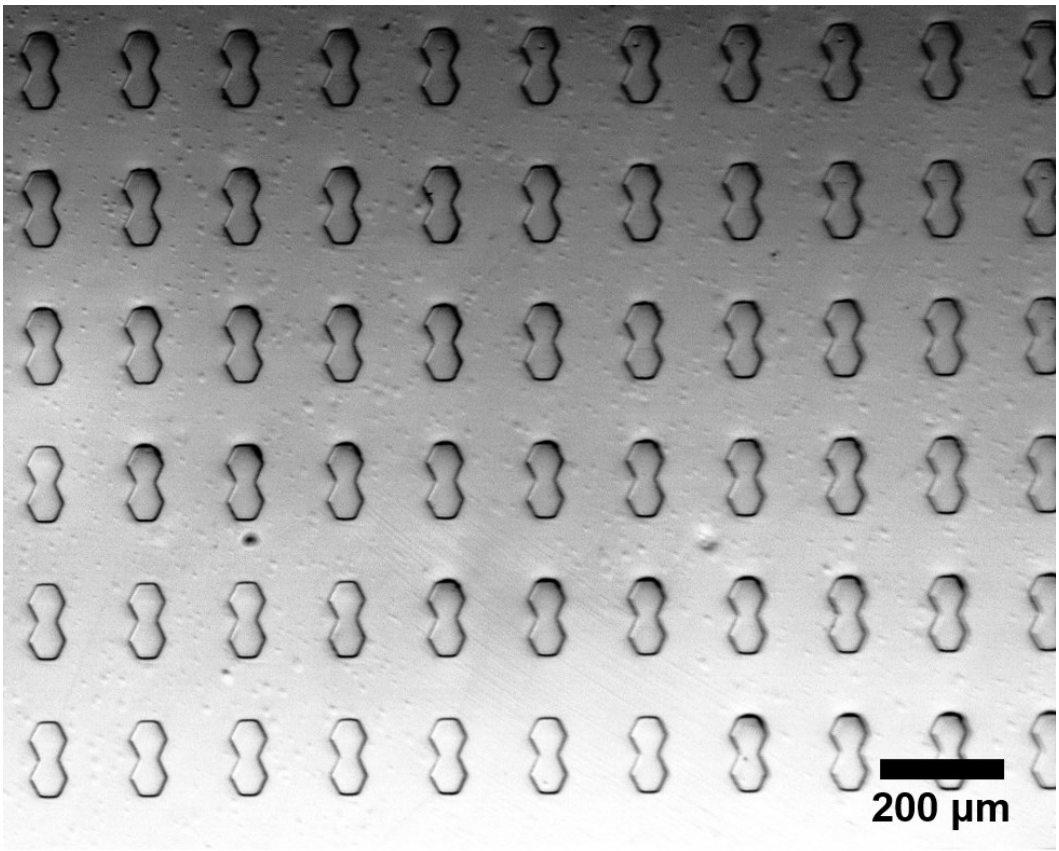

Figure S25. Stereoscopic image of a PDMS stamp used for microcontact printing.

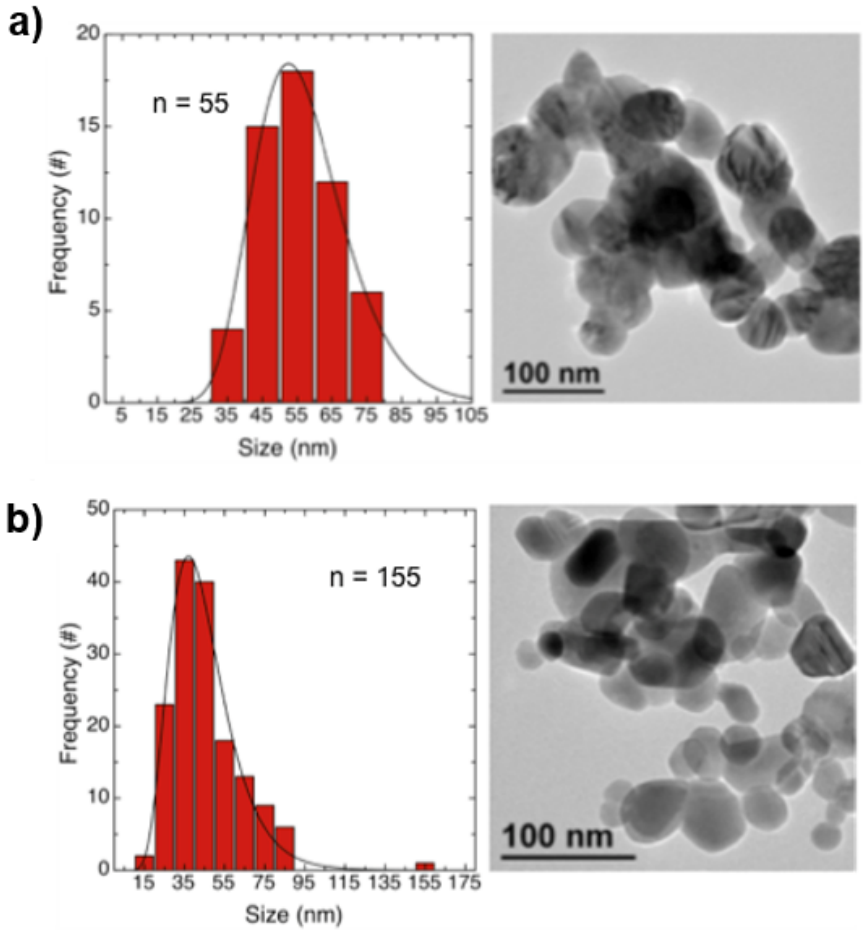

Figure S26. Representative electron microscopy images and primary particle size distributions of commercially available ENM. a) The mean Feret diameter of the measured CuO primary particles (*n*= 55) as measured by transmission electron microscopy (TEM) was 50 nm. b) The mean Feret diameter of the measured ZnO primary particles (*n*= 155) as measured by TEM was 46 nm.

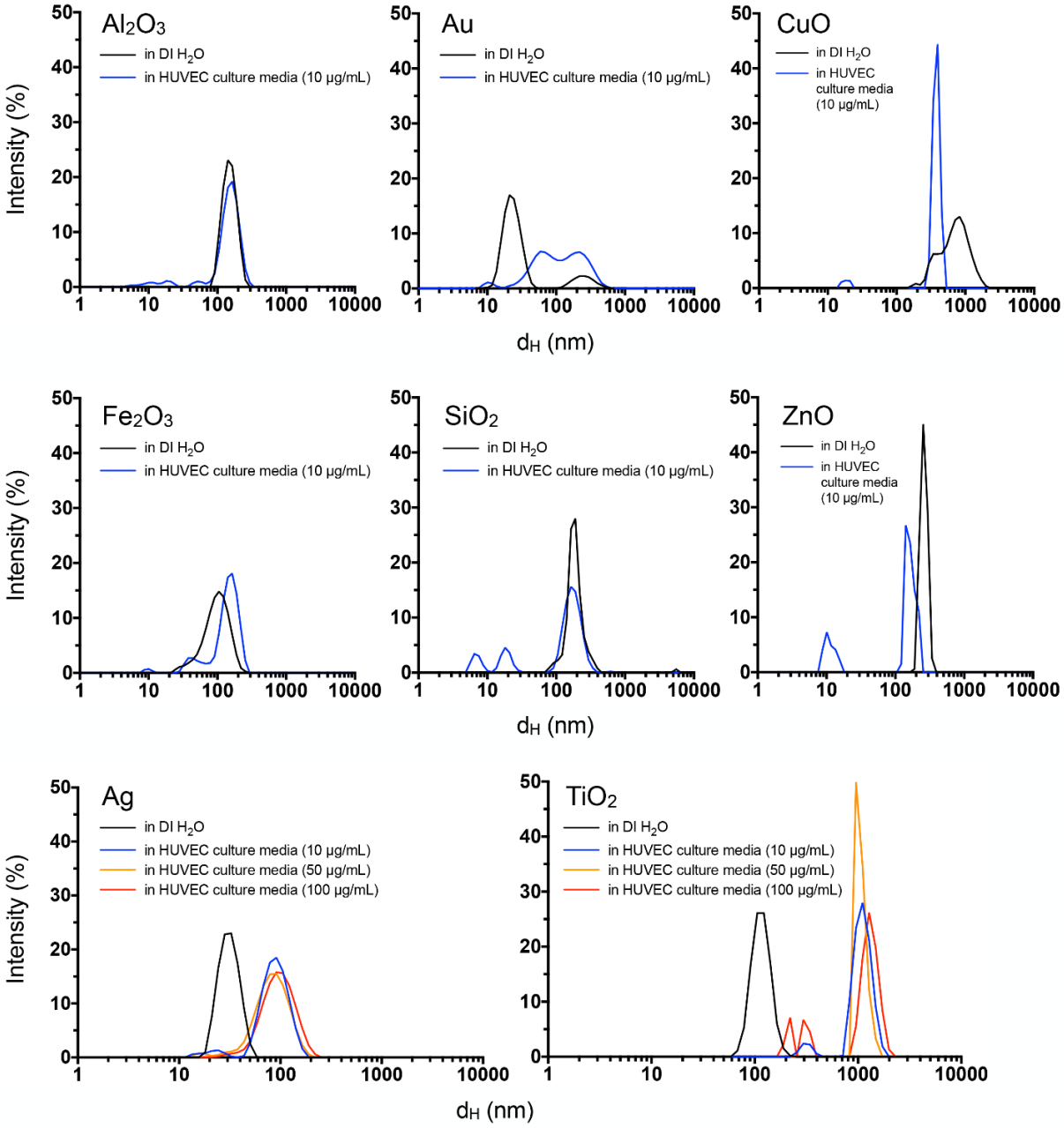

Figure S27. Intensity-weighted hydrodynamic size (d_H) distributions of the ENM used in this study as measured by dynamic light scattering (DLS). Dispersion in deionized water at 500 µg/mL (—) by cup-horn sonication based on their respective DSE_{cr} values; dispersion in HUVEC culture media at 10 µg/mL (—), 50 µg/mL (—), and 100 µg/mL (—).

Table S1. Summary of physical properties of CuO and ZnO. ρ, density of primary particle; SSA, specific surface area as measured by nitrogen adsorption/Brunauer-Emmett-Teller (BET) method; d_{BET}, d_{EM} and d_{XRD}, primary particle size as measured by BET, electron microscopy, and XRD, respectively.

		Primary Particle Size				Shape Factors			Crystal Structure	
ENM	**ρ (g/cm^3)**	**SSA ($m^2\ g^{-1}$)**	**d_{BET} (nm)**	**d_{EM} (nm)**	**d_{XRD}, (nm)**	**aspect ratio**	**circularity**	**roundness**	**crystal system**	**crystallinity**
CuO	6.1531 ± 0.0027	13.77 ± 0.68	70.90 ± 3.54	50.24 ± 10.99	25.8	1.345 ± 0.202	0.925 ± 0.037	0.759 ± 0.107	monoclinic tenorite	**73.1**
ZnO	6.1547 ± 0.0064	15.95 ± 0.80	61.24 ± 3.06	45.7 ± 17.4	27.9	1.230 ± 0.148	0.944 ± 0.025	0.823 ± 0.090	hexagonal zincite	**86.2**

Table S2. Summary of chemical and biological properties of CuO and ZnO. XPS, X-ray photoelectron spectroscopy; ICP-MS, inductively-coupled plasma mass spectrometry. *Elemental plus organic carbon content; †Pharmacopeia Protocol for Sterility WHO Document QAS/11.413 FINAL.

	Elemental Composition				Biological Characterization	
ENM	**Trace Metal Analysis (%)**	**Carbon Content* (w/w %)**	**Stoichiometry by XPS**	**Stoichiometry by ICP-MS**	**Recombinant Factor C (EU/mg)**	**Sterility† (bacteria/mg)**
CuO	98.21 ± 6.11 Cu	0.209 ± 0.136	$CuO_{1.01}$	$CuO_{1.41}$	2.141	0
ZnO	99.66 ± 3.60 Zn	0.158 ± 0.125	$ZnO_{0.98}$	$ZnO_{0.99}$	4.168	0

References

1. M.-A. P. Bray, W. J. Adams, N. A. Geisse, A. W. Feinberg, S. P. Sheehy and K. K. Parker, *Biomaterials*, 2010, **31**, 5143-5150.
2. S. V. Costes, D. Daelemans, E. H. Cho, Z. Dobbin, G. Pavlakis and S. Lockett, *Biophys J*, 2004, **86**, 3993-4003.
3. E. M. M. Manders, F. J. Verbeek and J. A. Aten, *Journal of Microscopy*, 1993, **169**, 375-382.